Sustainability & Circularity NOW

Entirely biomass-derived hydrogel composites for possible applications in drug delivery

Megan M Fitzgerald, Melissa Morgan, Francesca M Kerton.

Affiliations below.

Abstract:
Entirely biomass-based chitosan-alginate hydrogel composites were prepared using mussel-derived calcite. Composite hydrogel beads were prepared with 0.0 wt%, 1.0 wt% and 2.5 wt% calcite, and were characterized using IR spectroscopy, scanning electron microscopy (SEM), and thermogravimetric analysis (TGA). Diameters of beads were measured to ensure uniform preparation. The swelling behavior of beads were tested in 0.1 M HCl, 0.1 M potassium phosphate buffer and deionized water at 37 °C. Beads containing calcite were found to have significantly less swelling ability in 0.1 M HCl and deionized water, but in 0.1 M potassium phosphate buffer no change in swelling ability was observed for beads containing zero calcite compared with those containing calcite. Encapsulation efficiency (EE) measurements of methylene blue, as a model drug, showed that 0.0 wt% calcite beads had an EE of 80.8% and those containing calcite had lower EE: 60.7% (1.0 wt% calcite) and 71.6% (2.5 wt% calcite). Methylene blue release in a surrogate gastric environment (0.1 M HCl followed by 0.1 K buffer) showed that 0.0 wt% calcite beads had the least controlled release whereas those containing calcite showed controlled release. Drug release results were found to be significant through a one-way ANOVA test ($p < 0.05$).

Corresponding Author:
Prof. Francesca M Kerton, Memorial University of Newfoundland, Department of Chemistry, Core Science Facility, A1C 5S7 St. John's, Canada, fkerton@mun.ca

Contributors' Statement: Conceptualization: M. M. Fitzgerald, F. M. Kerton; Methodology: M. M. Fitzgerald, M. A. Morgan, F. M. Kerton; Data Collection: M. M. Fitzgerald, M. A. Morgan; Analysis and Interpretation of Data: M. M. Fitzgerald, M. A. Morgan, F. M. Kerton; Statistical Analysis: M. M. Fitzgerald, F. M. Kerton; Drafting the Manuscript: M. M. Fitzgerald, M. A. Morgan, F. M. Kerton; Critical Revision of Manuscript: F. M. Kerton; Resources, Funding, Administration and Supervision: F. M. Kerton

Affiliations:
Megan M Fitzgerald, Memorial University of Newfoundland, Department of Chemistry, St. John's, Canada
Melissa Morgan, Memorial University of Newfoundland, Department of Chemistry, St. John's, Canada
Francesca M Kerton, Memorial University of Newfoundland, Department of Chemistry, St. John's, Canada

Thieme

Entirely biomass-derived hydrogel composites for possible applications in drug delivery.

Megan M. Fitzgerald, Melissa A. Morgan, Francesca M. Kerton*

Department of Chemistry, Memorial University of Newfoundland, St. John's, NL, Canada A1B 3X7

*Corresponding author: fkerton@mun.ca

Abstract

Entirely biomass-based chitosan-alginate hydrogel composites were prepared using mussel-derived calcite. Composite hydrogel beads were prepared with 0.0 wt%, 1.0 wt% and 2.5 wt% calcite, and were characterized using IR spectroscopy, scanning electron microscopy (SEM), and thermogravimetric analysis (TGA). Diameters of beads were measured to ensure uniform preparation. The swelling behavior of beads were tested in 0.1 M HCl, 0.1 M potassium phosphate buffer and deionized water at 37 °C. Beads containing calcite were found to have significantly less swelling ability in 0.1 M HCl and deionized water, but in 0.1 M potassium phosphate buffer no change in swelling ability was observed for beads containing zero calcite compared with those containing calcite. Encapsulation efficiency (EE) measurements of methylene blue, as a model drug, showed that 0.0 wt% calcite beads had an EE of 80.8% and those containing calcite had lower EE: 60.7% (1.0 wt% calcite) and 71.6% (2.5 wt% calcite). Methylene blue release in a surrogate gastric environment (0.1 M HCl followed by 0.1 K buffer) showed that 0.0 wt% calcite beads had the least controlled release whereas those containing calcite showed controlled release. Drug release results were found to be significant through a one-way ANOVA test ($p < 0.05$). TGA data show that SC levels in beads after placement in a surrogate gastric fluid (0.1 M HCl) are significantly reduced due to the reaction between calcite and HCl.

Keywords:

Biomaterials

Renewable

Calcium carbonate

Blue economy

Biomass

Polysaccharides

Drug release

Significance

- Renewable feedstocks sourced from the oceans are often overlooked compared with biomass grown on land. This includes materials isolated from seaweed (algae) and waste streams for seafood processing.
- Calcium chloride typically used to crosslink alginate chains in hydrogels can be replaced with calcium chloride that can be entirely bio-sourced.
- This study shows that composite materials typical of those used in drug delivery applications could potentially release APIs more slowly if biogenic calcium carbonate is incorporated.

Introduction

Hydrogels are cross-linked polymer matrices that are insoluble in water, yet incredibly hydrophilic.[1–3] Their ability to retain large volumes of water make hydrogels relatively compatible with bodily tissues, thus, hydrogels are used in the field of medicine.[2,4–6] One of the first hydrogels to be adapted for practical applications was poly(hydroxyethyl methacrylate) used in contact lenses.[1] Now, synthetic hydrogels are used in several common household items: polyvinyl alcohol (PVA) hydrogels are commonly used in children's diapers and feminine hygiene products due to their quick absorbance of water.[1] PVA hydrogels are also used in several biomedical applications, such as tissue engineering and wound dressings.[5–8] Polyethylene glycol (PEG) derivatives can be used for drug delivery; for example, Puranik *et al*. showed the effectiveness of hydrogels made from different poly(methacrylic acid *g*-polyethylene glycol) derivatives to improve the delivery of doxorubicin to intestinal cells.[9] Though these synthetic hydrogels are well-suited for their applications, most are not biodegradable, or require harsh reagents for synthesis. Thus, to increase biodegradability of the hydrogel and to decrease hazards associated with their preparation, natural polymers can be used to create hydrogels.

Natural hydrogels are a class of hydrogel materials made from biomass-based sources, such as starch[10], cellulose[1], alginate[11–14], chitosan[13,15,16], gelatin[2], and several others. Some hydrogels are made using a mixture of one or more polymers.[3,10,11] Often, when oppositely charged polysaccharides are mixed, this causes gelation and the formation of a water-insoluble hydrogel matrix.[3,4] It is worth noting that of the carbohydrates commonly used sodium alginate and chitosan are also both ocean-derived materials, Figure 1.
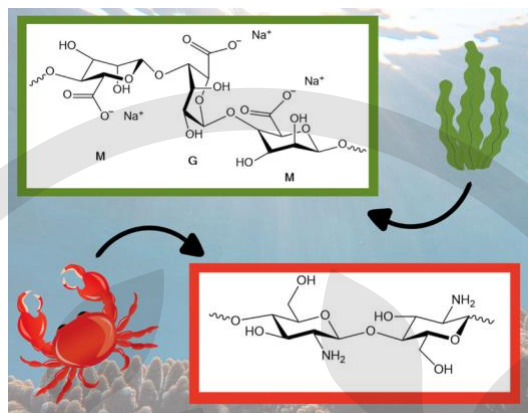
Figure 1: Sodium alginate and chitosan, and the ocean biomass from which they are derived. Prepared using Canva.com.

The fisheries are a prominent industry in coastal communities worldwide. Brown seaweed is also gaining popularity with some coastal entrepreneurs, as kelp farms are being developed as carbon capture strategies.[17] Goal 14 of the UN's Sustainable Development Goals (SDGs) is "Life Below Water" addresses the importance of protecting and nurturing the world's oceans and also making our fishing and aquaculture practices more sustainable.[18,19] In addition, SDG 12 pertains to "Responsible Consumption and Production" – this prioritizes a need for circular production methods and utilizing waste to create value-added products.[19,20] Waste reduction and valorizing waste from seafood processing pertains to goals 12 and 14 and is the driving force behind this work. The composite bead materials described herein use the following ocean-derived resources: calcite from waste blue mussel shells, chitosan from waste crustacean shells and sodium alginate from brown seaweeds.

Our group is not the only one interested in valorizing ocean biomass.[18,21–26] Moores and coworkers investigated the use of chitosan nanocrystals in alginate hydrogels as a drug delivery mechanism for fluorescein-labeled BSA as a model drug[27] - this inspired our choice of methylene blue as a model drug, as it is easily quantified using a colorimetric assay - similar to the fluorometric assay used by Moores and coworkers.[27] Chitosan-alginate hydrogels are of interest for drug delivery.[4,11,13,28] In this regard, it is important to note that chitosan is mucoadhesive when protonated, a property that makes the material a good candidate for drug delivery.[31] The lower digestive tract is covered in a mucosal layer; thus, chitosan has been a material of specific interest for drug delivery for colitis or colon cancer.[31,32]

3

There is some interest in combining organic polymers with inorganic material to create new hydrogel composites with interesting properties.[12,14,29–31] Calcium carbonate ($CaCO_3$) has also been combined with hydrogels to create regenerative tissues[5,7], as well as other applications such as wound dressings.[33] $CaCO_3$ is one of the most abundant natural minerals in the world, it is a key component in bones, teeth, exoskeletons, and mollusc shells. Blue mussel (*M. edulis*) shells are an excellent source of biogenic $CaCO_3$ ($CaCO_3$ synthesized by a living organism), a material with many practical applications. Shells are composed of two different biogenic $CaCO_3$ polymorphs: calcite and aragonite.[20,34,35] Calcite makes up the prismatic outer layer of the *M. edulis* shell, whereas the inner layer is made of nacreous aragonite - these two layers are separated by an organic matrix.[20,24,34]

By removing the protein and decomposing the organic matter of the shell, a procedure that was established by Murphy and coworkers, these two biomineral layers can be separated.[20,24,34] An unusual calcite material that was soft, malleable, and water-absorbent was also discovered and termed "soft calcite" (SC).[34] Acetic acid was used in dilute concentrations to generate SC and also forms calcium acetate as a by-product, Figure 2.
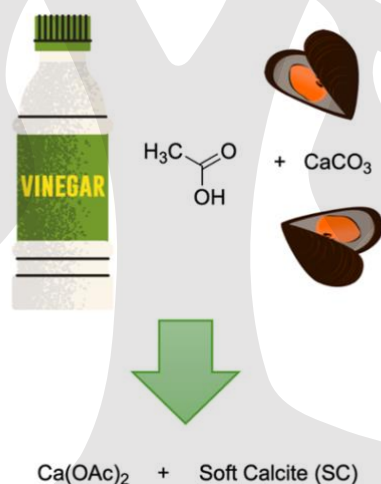

Figure 2: Materials found in some households, vinegar and mussel shells, can be used to make soft calcite.

Dilute acetic acid (vinegar) is also biomass-derived. There are several different ways in which acetic acid can be obtained from biomass industrially.[37,38] The concentration of acetic acid used to generate SC is similar to that of household vinegar, which can be obtained by the

fermentation of starches and sugars, then the consumption of ethanol by bacteria to produce acetic acid.[36,37,38] Inspired by an increased interest in valorizing ocean biomass waste, this work seeks to further examine possible biomedical applications of SC by creating SC-containing hydrogel beads, and using the calcium acetate produced during SC preparation as the crosslinking-agent in alginate hydrogel formation.

Results and Discussion

Soft calcite was obtained using the preparation method established by Murphy *et al.*[24,34] A photo and SEMs of SC are shown in Figure 3.
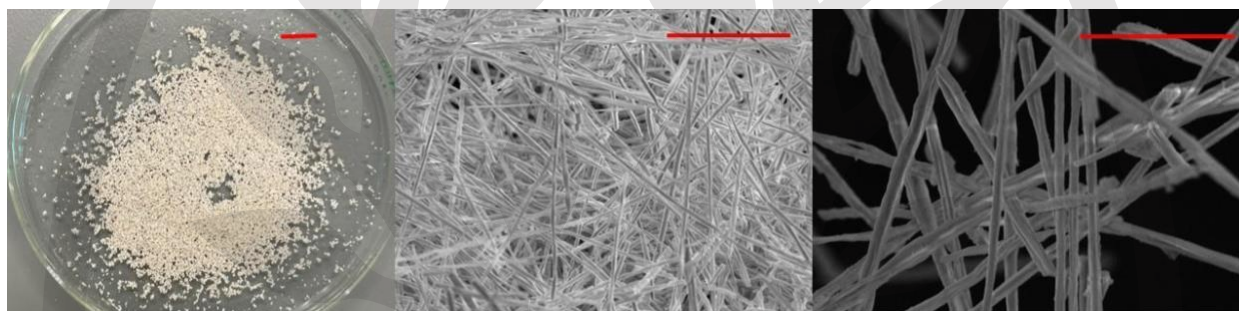

Figure 3: Left to right: (i) photo of SC on a watch glass taken using a cell phone camera, scale bar indicates 10 mm; (ii) SEM of SC, scale bar indicates 50 µm; (iii) SEM of SC, scale bar indicates 10 µm.

SC was incorporated into beads by mixing it into the 1.0 w/v% chitosan solution, with calcium acetate, before adding this mixture dropwise to the coagulation solution containing sodium alginate (see Experimental Section for more details). Beads were created with a chitosan core, containing SC, and an alginate outer layer (Figure 4). It should be noted that 0.0 wt% SC, 1.0 wt% SC, and 2.5 wt% SC refers to the wt% of SC added to the chitosan portion of each type of chitosan-alginate-SC beads, not the entire bead itself. Photos of beads made using 0.0 wt%, 1.0 wt% and 2.5 wt% SC are shown in Figure 5.
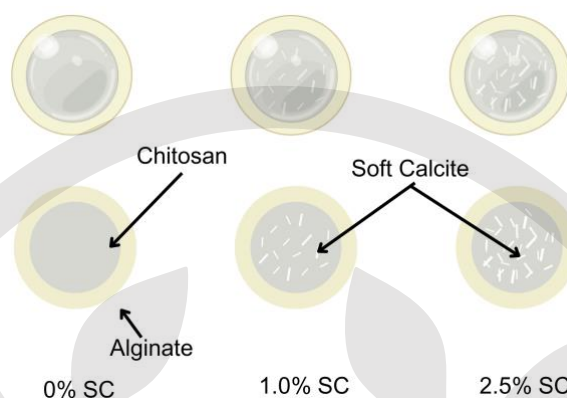
Figure 4: Graphical representation of 0.0 wt% SC, 1.0 wt% SC and 2.5 wt% SC beads, inner chitosan layer and outer alginate layer indicated. Created using biorender.com and canva.com.
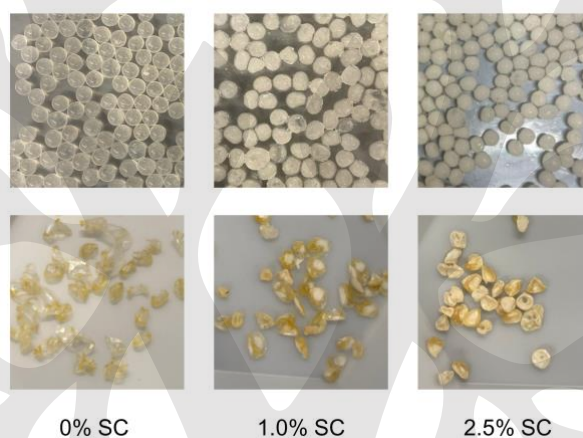

Figure 5: Photos of chitosan-alginate beads containing 0.0 wt% SC, 1.0 wt% SC, and 2.5 wt% SC in the chitosan centre. Top row: hydrated beads, bottom row: beads, after air-drying in fume hood for 18-20 h.

Chitosan-alginate beads are typically prepared using calcium chloride solutions to provide the Ca^{2+} ions necessary for gelation of alginate.[39,40] Calcium acetate (generated from treating mussel shells with acetic acid) was used as a calcium ion source in the current study. Treating mussel shells using the method from Murphy and coworkers, which utilizes 75 mL of 5% v/v acetic acid, and 5.0 g of the calcite layers of mussel shells produces approximately 4.4 g of calcium acetate monohydrate (referred to as calcium acetate herein). This further circularizes the method of preparing SC and preparing hydrogel beads by reducing waste. Adding 3% w/v calcium acetate to the chitosan solution led to the synthesis of firmer, more robust beads, whereas using 0-2% w/v calcium acetate led to the production of soft, sticky beads that broke upon any physical stress applied. Gelation occurs due to the presence of many α-L-guluronic

6

acid residues within the sodium alginate polymer chain, referred to as G-blocks.[12,39,40] The torsion about the β-glycosidic linkage between residues in G-blocks results in the formation of an egg-box structure with a Ca^{2+} ion, calcium alginate, which leads to formation of a much firmer hydrogel.[12,40,41]

Beads were made containing a chitosan inner layer and alginate outer layer. 1.0% w/v chitosan containing 3.0% w/v calcium acetate and either 0.0 wt%, 1.0 wt%, or 2.5 wt% SC were dropped into a coagulation solution containing 2.0% w/v sodium alginate. Using concentrations of sodium alginate greater than 2.0% w/v were attempted, however, this led to the formation of beads without uniform shape or diameter. Creating beads of relatively uniform shape and diameter were important to data collection for this study, as drug loading and drug release studies were performed on a sample of specific mass, thus, the number of beads within that specific mass had to be similar. It was found that the addition of SC to beads did not change the diameter of the bead itself upon synthesis. Mean diameter and standard deviation of diameter of each type of bead is reported in Table 1.

Table 1: Mean and standard deviation of diameters of 0.0 wt% SC, 1.0 wt% SC and 2.5 wt% SC beads.

Bead	Mean Diameter ($\bar{x}$) (mm)	Standard Deviation (mm)	N
0.0 wt% SC	6.41	0.47	20
1.0 wt% SC	6.19	0.49	20
2.5 wt% SC	6.59	0.44	20

Comparison of SEM images of cross-sections of 0.0 wt% and 1.0 wt% SC beads indicate the presence of soft calcite in the middle of the bead (Figure 6). Cross-section images also show the inner chitosan layer and outer alginate layer; yellow markings indicate the interface of both polymers. White matter in the middle of the bead, as well as the appearance of crystalline structures, indicates the incorporation of SC within the chitosan layer of the bead. The structure of the SC is also maintained within the centre of the bead, and is located only within the chitosan component.
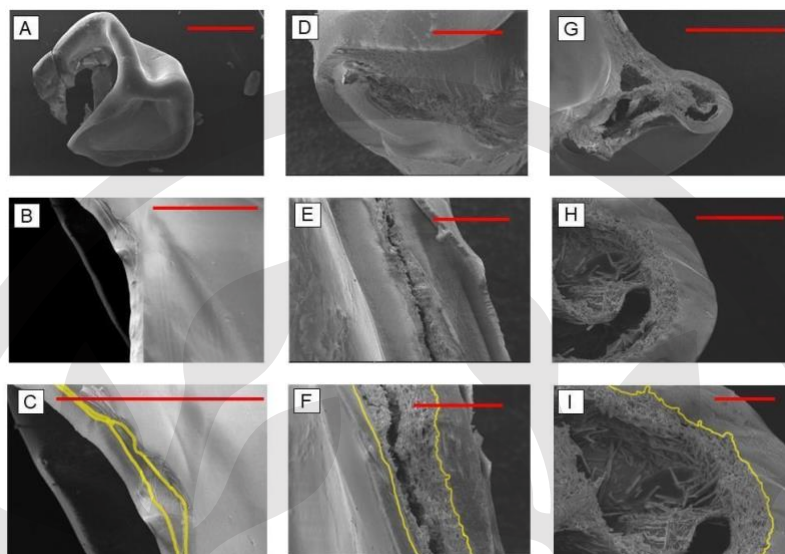
Figure 6: SEM images of 0.0 wt% SC beads (A-C) scale bars indicate 1 mm, 400 um, and 100 um, respectively. 1.0 wt% SC beads (D-F), scale bars indicate 100 um, 100 um, and 100 um, respectively. 2.5 wt% SC beads (G-I), scale bars indicate 500 um, 100 um, and 50 um, respectively. Yellow markings within beads indicate the intersection of the chitosan inner layer and the alginate outer layer.
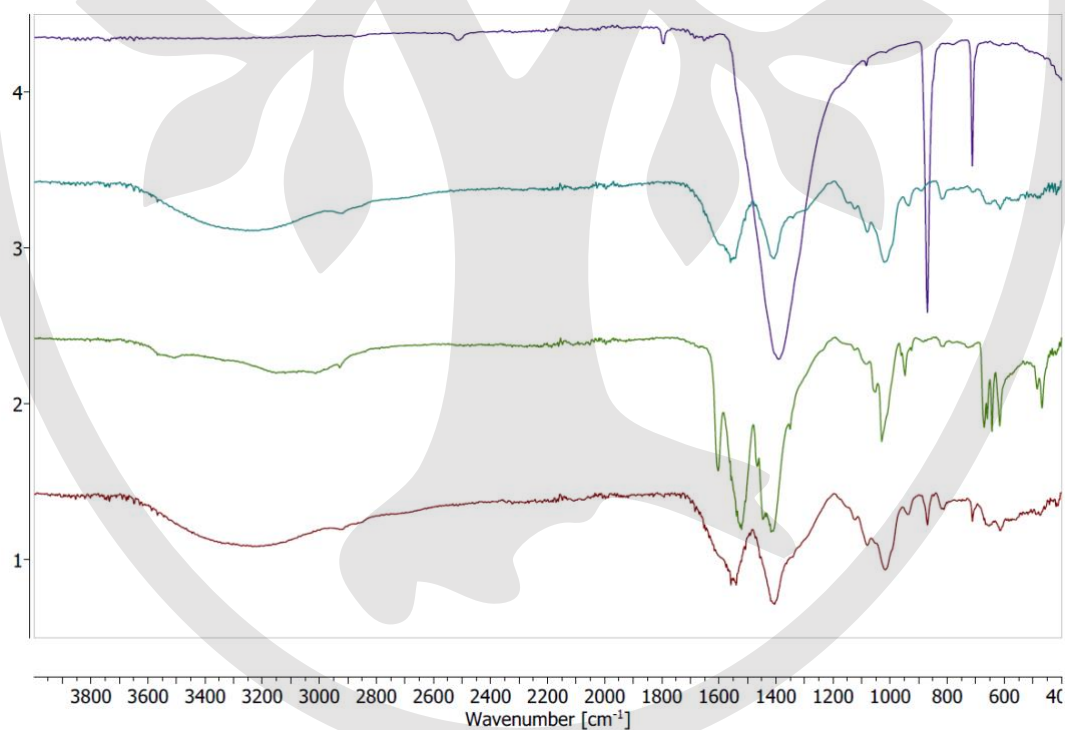

Figure 7: FT-IR spectra of (4) SC, (3) 0.0 wt% SC beads, (2) 1.0 wt% SC beads, (1) 2.5 wt% SC beads.

Dried beads were characterized using IR spectroscopy (Figure 7). Sodium alginate and chitosan FT-IR spectra both contain broad peaks at 3248 cm^{-1} and 3287 cm^{-1} respectively, correlated to hydroxyl group stretches (Figure S1 & S2, Table S1 & S2). The IR spectrum of sodium alginate (Figure S2) contains peaks at 1593 cm^{-1} and 1403 cm^{-1}, which can be attributed to the asymmetric and symmetric stretches (respectively) of the carboxylic acid groups.[14] In addition, a sharp peak at 1020 cm^{-1} indicates the presence of C-O stretches within the rings of the polymer.[40,41] A peak at 814 cm^{-1} also results from C-O stretches - in particular, the glycosidic links between β-D-mannuronic acid and α-L-guluronic acid residues.[40,42] For comparison, the IR spectrum of high molecular weight chitosan can be found in Figure S1 and Table S1. A sharp peak at 1636 cm^{-1} can be attributed to the -NH stretching of chitosan, 1060 cm^{-1} was attributed to the C-N bend on chitosan as well.[43,44]

The spectrum of SC (Figure 7, Spectrum 4) contains three major peaks – 1390 cm^{-1} corresponds to the v^3 band of CO_3^{2-}, specifically the COO$^-$ symmetric stretch. 869 cm^{-1} is attributed to the v^2 band - CO_3^{2-} asymmetric stretch and 712 cm^{-1} can be attributed to the v^4 band of CO_3^{2-}, the symmetric stretch.[24,34] As expected, the spectra of beads show no significant shifts in frequency for the bands associated with biopolymers compared with the spectra of sodium alginate and chitosan – this indicates that the polymer is largely unchanged, with the exception of the interaction of alginate C=O groups with NH_4^+ groups on chitosan, and Ca^{2+} ions. However, as wt% of SC increases, peaks at 869 cm^{-1} and 712 cm^{-1} increased in intensity. This demonstrates the incorporation of SC into the bead. It should be noted that the spectrum of the 1.0 wt% SC beads includes a peak at 1602 cm^{-1} which can be attributed to the chitosan within the bead, specifically, the C=O stretches of residual amide groups.[43,44] In the 0.0 wt% SC and 2.5 wt% SC beads, a weak, rounded peak can also be seen in the same region. This is a result of heterogeneity within samples.
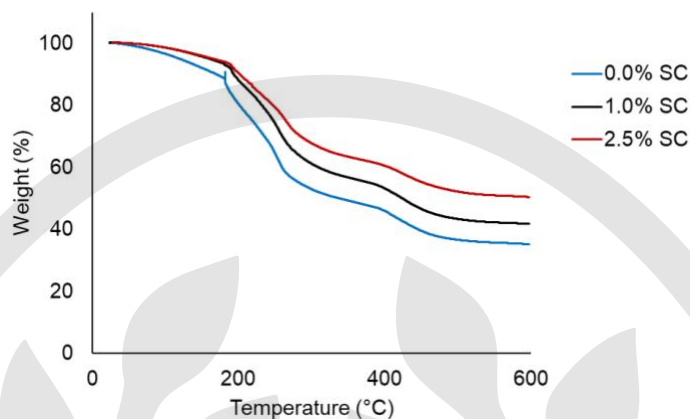
Figure 8: Thermograms of 0.0 wt% SC, 1.0 wt% SC, and 2.5 wt% SC beads.

TGA measurements were performed on sodium alginate, high MW chitosan, SC (Figures S3, S4, S5, with corresponding Tables S3, S4, S5) and the beads formed utilizing those materials (Figure 8 and Table 2).

Table 2: TGA weight loss percentage at certain temperature ranges for 0.0 wt% SC, 1.0 wt% SC, 2.5 wt% SC.

	Weight loss percent across selected T range, %			Total weight loss, %
SC Loading, wt%	25 – 180 °C	180 – 300 °C	300 – 600 °C	25 – 600 °C
0.0	8.41	38.94	13.31	60.66
1.0	7.67	31.68	14.98	54.26
2.5	6.88	26.53	12.27	45.68

Thermograms of all beads showed three weight loss events, which were assigned based on temperature and literature precedent. The first weight loss occurred from 25°C – 180 °C, which results from loss of moisture. The second event, happening from 180 °C – 300 °C, indicates initial decomposition of the biopolymers via breaking of ether linkages of both the chitosan and alginate polymers. The final event indicates complete degradation of the biopolymers to form a carbon-rich char. At 600 °C, the remaining mass can be attributed to the presence of decomposed organic matter and SC. $CaCO_3$ degrades at temperatures above 600 °C, resulting in the formation of CO_2 and CaO, therefore, it can be assumed that the SC is still present at 600 °C. Consequently, 2.5 wt% SC beads were shown to have the largest mass remaining after

10

heating to 600 °C, whereas 1.0 wt% SC beads had the next largest, and 0.0 wt% had the lowest mass remaining after heating. All beads yield some residues after heating as TGA was performed under nitrogen.

Swelling ratio is a measure of the volume of solution that a hydrogel can retain, and can change depending on temperature, dissolved solutes, or pH.[2,12] Three solutions were tested to determine swelling within biologically-relevant solutions - 0.1 M HCl (surrogate gastric fluid), 0.1 M potassium phosphate buffer (K buffer, surrogate intestinal fluid), and deionized water, all at biologically-relevant temperature, 37 °C. Swelling ratio is relevant to drug delivery as water can move easily over cellular membranes, thus, if hydrogels can retain larger volumes of solution, drug delivery may be more effective.
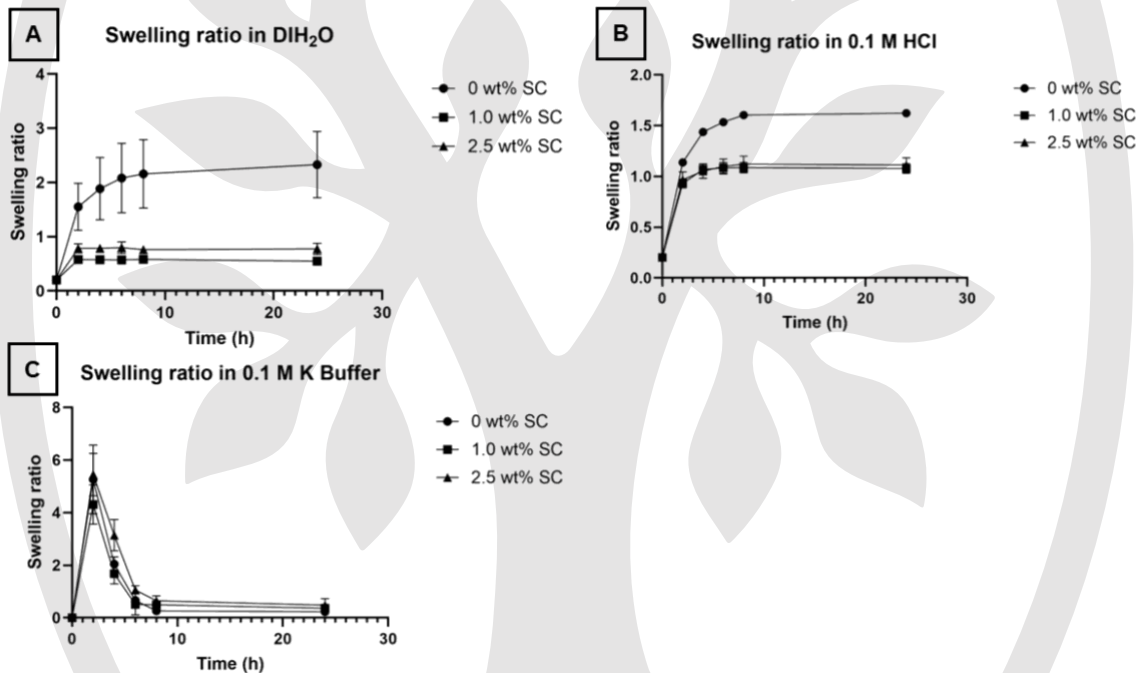
Figure 9: Swelling ratio of 0.0 wt% SC, 1.0 wt% SC and 2.5 wt% SC beads in A) deionized water B) 0.1 M HCl and C) 0.1 M potassium phosphate buffer (K buffer).

All beads suspended in 0.1M HCl showed a gradual increase in swelling ratio over a 24 h period. 0.0 wt% SC beads showed the greatest swelling ratio for each allotted time, while the 1.0 wt% and 2.5 wt% SC beads showed a similar trend to each other in terms of swelling ratio increase over time (Figure 9). This can be attributed to the dissolution of SC within the bead in the acidic media. This was evidenced using TGA, which confirmed no SC remained in beads after suspension in 0.1 M HCl for 24 h (Figure S7 and Table S7). Beads were heated in an N_2

atmosphere to 600 °C, as such, after being heated to 600 °C, the remaining material that would make up the final weight % would consist of $CaCO_3$ and decomposed organic matter. Final weight % values for all bead samples (0, 1.0 and 2.5 wt% SC) suspended in 0.1 M HCl for 24 h were found to be similar after heating to 600 °C, indicating only decomposed organic matter remained. Resulting final weight% values for beads suspended in 0.1 M HCl for 24 h differed from those of untreated beads. Results were also found to be significant through a one-way ANOVA test ($p<0.05$).

Submerging the three types of bead (0.0 wt%, 1.0 wt% and 2.5 wt% SC) in 0.1 M K-buffer (pH 7.4) showed no significant difference in their swelling ratios over time as indicated by a one-way ANOVA test ($p>0.05$) (Figure 9). Mass loss from all three bead types suspended in K-buffer results from the dissolution of the alginate biopolymer. Phosphate ions compete with carboxylic acid groups on the alginate polymer to bind with Ca^{2+} in solution, thus removing the calcium ion from the egg-box structure, reforming water-soluble alginate.[39] TGA data above indicates that 2.5 wt% SC beads contain a smaller fraction of organic matter in comparison to 1.0 wt% SC beads and 0.0 wt% SC beads, thus, it would be expected that the swelling capacity of 2.5 wt% SC beads would be less than 1.0 wt% SC beads, rather than what was seen in the results. The results observed may be attributed to free Ca^{2+} ions forming via dissolution of SC present within the centre of the bead, which could act as a Ca^{2+} ion source for any unbound G-residues in the alginate layer.

Swelling of beads in deionized water was found to be greatest for 0.0 wt% SC beads, followed by 2.5 wt% SC beads and then 1.0 wt% SC beads. Results were found to be significant through a one-way ANOVA test ($p<0.05$). As previously mentioned, the polysaccharide content of the 1.0 wt% SC bead is much lower than the 0.0 wt% SC bead, and lower still in the 2.5 wt% SC bead. Though the inorganic material is present, SC had been identified by Murphy *et al.* as an absorbent material.[24,34] Thus, the water absorbance of the SC material in the 2.5 wt% SC bead could potentially contribute to its larger capacity for deionized water absorption compared with the 1.0 wt% SC beads.

Encapsulation efficiency[3] of MB (EE, Figure 10, left) for the 0.0 wt% SC bead was found to be 80.8%, whereas the EE for 1.0 wt% SC bead was 60.7%, and the EE for the 2.5 wt% SC bead was found to be 71.6%. The EE of the 0.0 wt% SC bead was found to be greater than either SC-containing bead, which could be attributed to the fact that the inorganic SC is a solid material and takes up space that could otherwise be occupied by the water-solvated MB between biopolymer chains within the hydrogel. The difference in EE between 1.0 wt% SC and

12

2.5 wt% SC may be attributed to an interaction between the cationic dye and the surface of the calcite.[45]
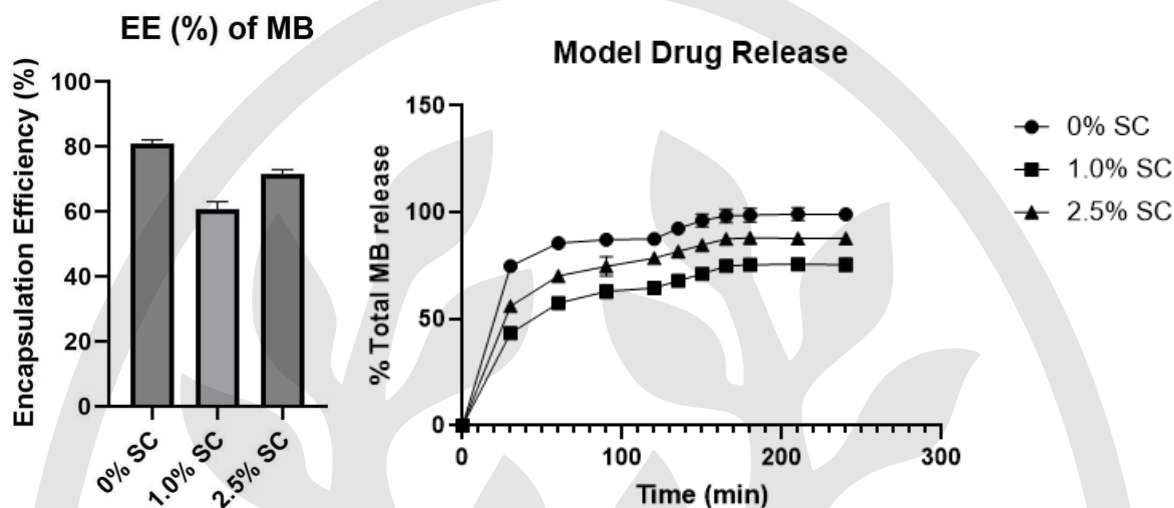

Figure 10: Left: Encapsulation efficiency of model drug (MB). Right: Drug release of model drug (MB) in surrogate gastric fluid (0.1 M HCl, 0-120 min) and surrogate intestinal fluid (0.1 K buffer, 120-240 min).

Beads that were loaded by absorption were then subject to drug release in a surrogate gastric environment (0.1 M HCl, pH 1.2, without enzymes) from 0-120 min.[13,39] HCl was then decanted off and replaced with 0.1 M potassium phosphate buffer (K buffer, pH 7.4, without enzymes) from 120-240 min.[13,39] Drug release is reported as a fraction of total MB that was loaded by absorption during the encapsulation efficiency procedure previously described. Surprisingly, 1.0 wt% SC beads showed a more controlled release compared with 2.5 wt% SC beads. This can be deduced from the graph as 1.0 wt% SC beads showed the smallest % of total loaded MB released reaching a maximum % release of 75.5% over the 240 min period, whereas 2.5 wt% SC beads reached a maximum of 87.8% and 0 wt% reached a maximum of 99.0% release. Results were found to be significant through a one-way ANOVA test ($p < 0.05$). Surprisingly, beads containing 1.0 wt% SC exemplified the most controlled release curve in comparison with 2.5 wt% SC beads, which was unexpected due to the lower SC loading and lower EE compared to the 2.5 wt% SC bead.

Conclusions

SC was successfully incorporated within chitosan-alginate beads, creating fully biomass-derived composite hydrogel materials. SEM and FT-IR were used to confirm the presence of SC within the 1.0 wt% and 2.5 wt% SC-containing hydrogel beads. Swelling behavior of beads in 0.1 M HCl and deionized water was significantly lower for chitosan-alginate beads containing SC compared with controls containing 0.0 wt% SC. However, swelling behavior of beads in the 0.1 M K buffer did not change upon the addition of SC. Encapsulation efficiency (EE) was found to be reduced upon the addition of SC compared with control materials. However, EE of 2.5 wt% SC beads was found to be higher than EE of 1.0 wt% SC beads. Drug release experiments showed that the addition of SC does make the release of MB from hydrogel beads significantly more controlled, meaning the portion (%) of encapsulated model drug released over time is lowered. The most controlled release was shown by the bead containing 1.0 wt% SC. Future directions of this work could include investigating the release of different model drugs in the same surrogate gastric environment.

Experimental Section

<u>Materials</u>

Chitosan (high molecular weight), alginate sodium salt (derived from brown algae), methylene blue, glacial acetic acid (99.9%, ACS grade) and ethanol (95%), were purchased from Sigma Aldrich Canada. Blue mussels were purchased from a local grocery store in St. John's, Newfoundland. Deionized water was used to create methylene blue solutions, acetic acid solutions, 0.1 M HCl, and 0.1M potassium phosphate buffer.

<u>Soft Calcite and Calcium Acetate</u>

Soft calcite (SC) was prepared in a similar way to that reported by Murphy et al.[24,34] After the removal of protein from blue mussel shells using a protease enzyme,[20,24] shells were heated at 220 °C for 72 h. Calcite and aragonite layers were then physically separated.[24,29] Calcite layers were treated with 5% v/v acetic acid in a ratio of 5.0 g of shell to 75.0 mL acetic acid, and shaken on a shaker-incubator at 25 °C, 100 rpm for 24 h.[24] After 24 h, the result of this process was a suspension of mussel shell fragments in a solution of dissolved calcium acetate.[20] The remaining unreacted shell residues were treated a second time with 5% acetic acid in a 5.0 g:75.0 mL ratio for an additional 24 h.[24,34] After 24 h, the flask contained a suspension of SC in a solution of calcium acetate. The suspension was filtered to collect SC, which was then washed

with ~50 mL of 95% ethanol, and dried at 50 °C for 16-20 h.[24,34] The calcium acetate solution was set aside to isolate solid calcium acetate, as described below.

Calcium acetate monohydrate was isolated from the decanted solution according to the procedure established by Murphy et al.[24] The solution was filtered to remove insoluble particles and treated with activated charcoal to remove dissolved impurities. The filtered solution was then boiled until water had evaporated. The result was a white powder - calcium acetate monohydrate.[24]

Hydrogel bead preparation

Beads were made by preparing a 5% w/v bulk solution of sodium alginate, which was later diluted to 2.0% w/v on day of use. A 1.0% w/v solution of high molecular weight chitosan was prepared in 1.0% v/v acetic acid solution. On the day of bead preparation, 30.0 mL chitosan solution was prepared containing 3.0% w/v calcium acetate (0.3 g per bead preparation) and either 0 wt%, 1.0 wt% or 2.5 wt% SC.
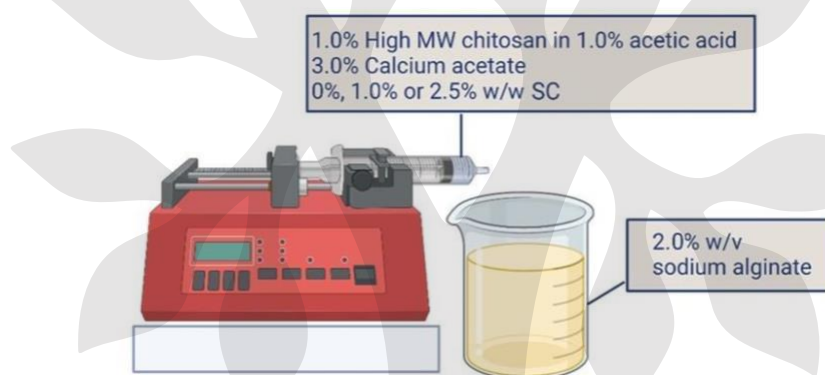

Figure 11: Schematic of hydrogel bead preparation, prepared using biorender.com

The chitosan mixture was loaded into a 20 mL polyethylene syringe (Henke-Sass Wolf, Germany) without a needle. A Chemyx Fusion 200 dual syringe pump (Chemyx inc, USA), equipped with this single syringe was placed next to a beaker full of coagulation solution (2.0% w/v sodium alginate), Figure 11. The chitosan mixture was added dropwise into the coagulation solution at a rate of 20 mL/hr. Resulting beads were stirred for an additional 20 min after the syringe was emptied to ensure gelation had occurred. The beads were collected by pouring the coagulation solution through a metal sieve and were then washed with deionized water (3 × 20 mL), and subsequently ethanol (3 × 20 mL). Beads were placed onto a glass petri dish and air-dried in a fume hood overnight (16-20 h).

Characterization of composite hydrogel beads

Bead diameter

Photos of hydrogel beads before drying were taken using a cell phone camera, containing a ruler for scale. Photos were uploaded to ImageJ, the diameter of 20 beads within the petri dish were collected. Mean and standard deviation of these measurements were calculated using Microsoft excel.

FT-IR Spectroscopy

Spectra were collected using a Bruker Alpha FT-IR spectrometer, using a single-bounce diamond ATR platform. Spectra were obtained with a scan range of 400-4000 cm^{-1} with 24 scans and a 4 cm^{-1} resolution.

Scanning Electron Microscopy (SEM-EDX)

Scanning electron micrographs (SEM) were collected using an FEI MLA 650FEG instrument equipped with an electron backscattering diffraction system and corresponding software. Samples were loaded onto carbon double-sided Pelco 12 mm diameter tabs. SC was spread onto carbon tabs, whereas beads were cut using a scalpel to obtain SEM of bead cross-sections. Experiments were performed under high vacuum with voltage of 5-10 kV and a working distance of 10-20 mm.

Thermogravimetric Analysis

A TA 850 thermogravimetric analyser was used to perform thermogravimetric analysis on each bead sample. Experiments were performed under N_2 atmosphere from room temperature to 600°C, with a heating rate of 10°C/min. Samples were analyzed on platinum pans.

Swelling Ratio

Experiments were performed in triplicate. 200 mg of dried beads were placed into a flask with 50.0 mL of deionized water, heated to 37 °C and shaken at 90 rpm in an incubator shaker (model: Eppendorf New Brunswick Innova 40/40R Benchtop).

After 2 h, 4 h, 6 h, 8 h, and 24 h, beads were removed from solution, dried with a Kimwipe, and mass was recorded. Masses were then used to determine swelling ratio (SR) using the equation below, in which M_t = mass of swollen beads at time t, M_d = mass of dried hydrogel beads:

$$SR = \frac{M_t - M_d}{M_d}$$

Experiments were repeated using 0.1 M HCl, and 0.1 M potassium phosphate buffer at 37 °C.
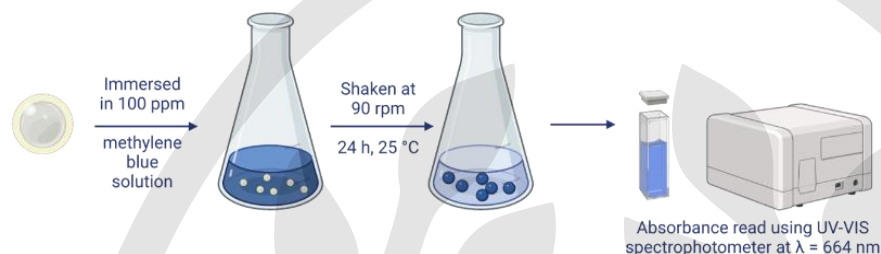
Methylene blue encapsulation efficiency

Figure 12: Schematic representation of loading of model drug (MB) within hydrogel beads, prepared using biorender.com

Experiments were performed in triplicate. MB was loaded into dried hydrogel beads by suspending 300 mg of beads in 50.0 mL MB solution (294 mg/mL), shaken at 90 rpm at 25 °C for 24 h, Figure 12. UV-VIS analysis was used to determine the amount of MB loaded into beads after the 24 h loading period. UV-VIS experiments were performed using a Cary60 UV-VIS spectrophotometer and polypropylene cuvettes.

Encapsulation efficiency was calculated using the following equation:

$$\%EE = \frac{M_t - M_f}{M_t} * 100\%$$

In which %EE is encapsulation efficiency (%), M_t = mass of total drug (g), and M_f = mass of free (non-encapsulated) drug (g).

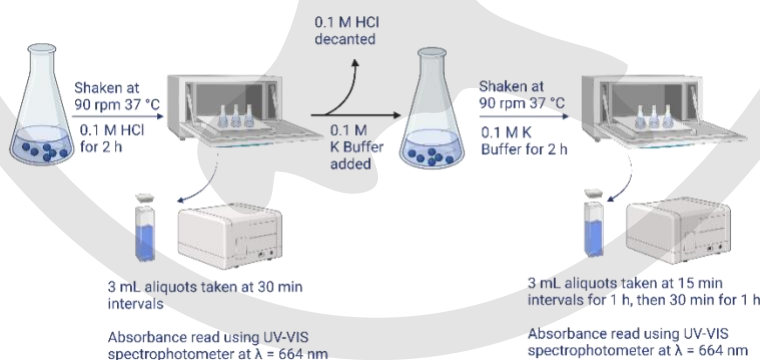Methylene blue release in surrogate digestive system

Figure 13: Schematic of MB drug release, prepared using Biorender.com.

17

Release of MB was observed in a simulated digestive system without enzymes, Figure 13. 300 mg of MB-loaded beads were suspended in 50.0 mL of surrogate gastric fluid (0.1 M HCl) for 2 h, in which 3.00 mL aliquots were removed and stored for UV-VIS analysis after 30, 60, 90, and 120 min. 3.00 mL aliquots of fresh solutions replaced those removed from the sample, and were accounted for during drug release calculations. The concentration of MB in these samples was determined as described above in encapsulation efficiency.

Statistical analysis:

Statistical analyses were performed using GraphPad Prism 10.2.2, using an XY table and a one-way ANOVA test.

Conflict of Interest

The authors declare that they have no conflict of interest.

References

1. Mondal, Md. I. H.; Haque, Md. O. Cellulosic Hydrogels: A Greener Solution of Sustainability. In *Cellulose-Based Superabsorbent Hydrogels*; Mondal, Md. I. H., Ed.; Polymers and Polymeric Composites: A Reference Series; Springer International Publishing: Cham, **2019**; pp 3–35.

2. Hoare, T. R.; Kohane, D. S. Hydrogels in Drug Delivery: Progress and Challenges. *Polymer* **2008**, *49* (8), 1993–2007.

3. Jing, H.; Huang, X.; Du, X.; Mo, L.; Ma, C.; Wang, H. Facile Synthesis of pH-Responsive Sodium Alginate/Carboxymethyl Chitosan Hydrogel Beads Promoted by Hydrogen Bond. *Carbohydr. Polym.* **2022**, *278*, 118993.

4. Phan, V. H. G.; Mathiyalagan, R.; Nguyen, M.-T.; Tran, T.-T.; Murugesan, M.; Ho, T.-N.; Huong, H.; Yang, D. C.; Li, Y.; Thambi, T. Ionically Cross-Linked Alginate-Chitosan Core-Shell Hydrogel Beads for Oral Delivery of Insulin. *Int. J. Biol. Macromol.* **2022**, *222*, 262–271.

5. Petrini, P.; Farè, S.; Piva, A.; Tanzi, M. C. Design, Synthesis and Properties of Polyurethane Hydrogels for Tissue Engineering. *J. Mater. Sci. Mater. Med.* **2003**, *14* (8), 683–686.

6. Visakh, P. M. Biomonomers for Green Polymers: Introduction. In *Bio Monomers for Green Polymeric Composite Materials*; John Wiley & Sons, Ltd, **2019**; pp 1–24.

7. Ren, B.; Chen, X.; Du, S.; Ma, Y.; Chen, H.; Yuan, G.; Li, J.; Xiong, D.; Tan, H.; Ling, Z.; Chen, Y.; Hu, X.; Niu, X. Injectable Polysaccharide Hydrogel Embedded with Hydroxyapatite and Calcium Carbonate for Drug Delivery and Bone Tissue Engineering. *Int. J. Biol. Macromol.* **2018**, *118*, 1257–1266.

8. Froelich, A.; Jakubowska, E.; Wojtyłko, M.; Jadach, B.; Gackowski, M.; Gadziński, P.; Napierała, O.; Ravliv, Y.; Osmałek, T. Alginate-Based Materials Loaded with Nanoparticles in Wound Healing. *Pharmaceutics* **2023**, *15* (4), 1142.

9. Puranik, A. S.; Pao, L. P.; White, V. M.; Peppas, N. A. In Vitro Evaluation of pH-Responsive Nanoscale Hydrogels for the Oral Delivery of Hydrophobic Therapeutics. *Ind. Eng. Chem. Res.* **2016**, *55* (40), 10576–10590.

10. Zhu, J.; Zhong, L.; Chen, W.; Song, Y.; Qian, Z.; Cao, X.; Huang, Q.; Zhang, B.; Chen, H.; Chen, W. Preparation and Characterization of Pectin/Chitosan Beads Containing Porous Starch Embedded with Doxorubicin Hydrochloride: A Novel and Simple Colon Targeted Drug Delivery System. *Food Hydrocoll.* **2019**, *95*, 562–570.

11. Hari, P. R.; Chandy, T.; Sharma, C. P. Chitosan/Calcium–Alginate Beads for Oral Delivery of Insulin. *J. Appl. Polym. Sci.* **1996**, *59* (11), 1795–1801.

12. Huang, Y.; Cao, L.; Parakhonskiy, B. V.; Skirtach, A. G. Hard, Soft, and Hard-and-Soft Drug Delivery Carriers Based on CaCO3 and Alginate Biomaterials: Synthesis, Properties, Pharmaceutical Applications. *Pharmaceutics* **2022**, *14* (5), 909.

13. Anal, A. K.; Stevens, W. F. Chitosan–Alginate Multilayer Beads for Controlled Release of Ampicillin. *Int. J. Pharm.* **2005**, *290* (1), 45–54.

14. Lai, W.-F.; Wong, E.; Wong, W.-T. Multilayered Composite-Coated Ionically Crosslinked Food-Grade Hydrogel Beads Generated from Algal Alginate for Controlled and Sustained Release of Bioactive Compounds. *RSC Adv.* **2020**, *10* (72), 44522–44532.

15. Coma, V. Recent Developments in Chitin and Chitosan Bio-Based Materials Used for Food Preservation. In *Polysaccharide Building Blocks*; John Wiley & Sons, Ltd, **2012**; pp 143–175.

16. Rhazi, M.; Tolaimate, A.; Habibi, Y. Interactions of Chitosan with Metals for Water Purification. In *Polysaccharide Building Blocks*; John Wiley & Sons, Ltd, **2012**; pp 127–141.

17. Bullen, C. D.; Driscoll, J.; Burt, J.; Stephens, T.; Hessing-Lewis, M.; Gregr, E. J. The Potential Climate Benefits of Seaweed Farming in Temperate Waters. *Sci. Rep.* **2024**, *14* (1), 15021.

18. Veríssimo, N. V.; Mussagy, C. U.; Oshiro, A. A.; Mendonça, C. M. N.; Santos-Ebinuma, V. de C.; Pessoa, A.; Oliveira, R. P. de S.; Pereira, J. F. B. From Green to Blue Economy: Marine

Biorefineries for a Sustainable Ocean-Based Economy. *Green Chem.* **2021**, *23* (23), 9377–9400.

19.   Mohan, C.; Robinson, J.; Vodwal, L.; Kumari, N. Chapter 16 - Sustainable Development Goals for Addressing Environmental Challenges. In *Green Chemistry Approaches to Environmental Sustainability*; Garg, V. K., Yadav, A., Mohan, C., Yadav, S., Kumari, N., Eds.; Advances in Green and Sustainable Chemistry; Elsevier, **2024**; pp 357–374.

20.   Murphy, J. N.; Schneider, C. M.; Mailänder, L. K.; Lepillet, Q.; Hawboldt, K.; Kerton, F. M. Wealth from Waste: Blue Mussels (Mylitus Edulis) Offer up a Sustainable Source of Natural and Synthetic Nacre. *Green Chem.* **2019**, *21* (14), 3920–3929.

21.   Kerton, F. M.; Liu, Y.; Omari, K. W.; Hawboldt, K. Green Chemistry and the Ocean-Based Biorefinery. *Green Chem.* **2013**, *15* (4), 860–871.

22.   Kerton, F. M.; Yan, N.; Overview of Ocean and Aquatic Sources for the Production of Chemicals and Materials. In *Fuels, Chemicals and Materials from the Oceans and Aquatic Sources*, 1st ed.; John Wiley & Sons: Newark, 2017; pp. 1-17

23.   Wyper, O. M.; Zendehboudi, S.; Kerton, F. M. The Sea's Best Kept Secret: The Use of Seaweed as a Source of Biohydrogen for Clean and Renewable Energy. *RSC Sustain.* **2024**, *2* (5), 1289–1299.

24.   Murphy, J. N. Adding Value to Waste from the Aquaculture Industry: The Development of Green Processing Technologies, Characterization, and Applications of Waste Blue Mussel Shells. Doctoral Thesis, Memorial University of Newfoundland, **2019**. https://research.library.mun.ca/14013/.

25.   Alphons Sequeira, R.; Mondal, D.; Prasad, K. Neoteric Solvent-Based Blue Biorefinery: For Chemicals, Functional Materials and Fuels from Oceanic Biomass. *Green Chem.* **2021**, *23* (22), 8821–8847.

26.   Amiri, H.; Aghbashlo, M.; Sharma, M.; Gaffey, J.; Manning, L.; Moosavi Basri, S. M.; Kennedy, J. F.; Gupta, V. K.; Tabatabaei, M. Chitin and Chitosan Derived from Crustacean Waste Valorization Streams Can Support Food Systems and the UN Sustainable Development Goals. *Nat. Food* **2022**, *3* (10), 822–828.

27.   Jin, T.; Liu, T.; Jiang, S.; Kurdyla, D.; Klein, B. A.; Michaelis, V. K.; Lam, E.; Li, J.; Moores, A. Chitosan Nanocrystals Synthesis via Aging and Application towards Alginate Hydrogels for Sustainable Drug Release. *Green Chem.* **2021**, *23* (17), 6527–6537.

28.   Tahtat, D.; Mahlous, M.; Benamer, S.; Khodja, A. N.; Oussedik-Oumehdi, H.; Laraba-Djebari, F. Oral Delivery of Insulin from Alginate/Chitosan Crosslinked by Glutaraldehyde. *Int. J. Biol. Macromol.* **2013**, *58*, 160–168.

29.   Li, Z.; Su, Y.; Xie, B.; Wang, H.; Wen, T.; He, C.; Shen, H.; Wu, D.; Wang, D. A Tough Hydrogel–Hydroxyapatite Bone-like Composite Fabricated in Situ by the Electrophoresis Approach. *J. Mater. Chem. B* **2013**, *1* (12), 1755–1764.

30.   Wang, X.; Wei, W.; Guo, Z.; Liu, X.; Liu, J.; Bing, T.; Yu, Y.; Yang, X.; Cai, Q. Organic–Inorganic Composite Hydrogels: Compositions, Properties, and Applications in Regenerative Medicine. *Biomater. Sci.* **2024**, *12* (5), 1079–1114.

31.   Yu, C.-Y.; Yin, B.-C.; Zhang, W.; Cheng, S.-X.; Zhang, X.-Z.; Zhuo, R.-X. Composite Microparticle Drug Delivery Systems Based on Chitosan, Alginate and Pectin with Improved pH-Sensitive Drug Release Property. *Colloids Surf. B Biointerfaces* **2009**, *68* (2), 245–249.

32.   Wu, T.; Yu, S.; Lin, D.; Wu, Z.; Xu, J.; Zhang, J.; Ding, Z.; Miao, Y.; Liu, T.; Chen, T.; Cai, X. Preparation, Characterization, and Release Behavior of Doxorubicin Hydrochloride from Dual Cross-Linked Chitosan/Alginate Hydrogel Beads. *ACS Appl. Bio Mater.* **2020**, *3* (5), 3057–3065.

33.   Azarian, M. H.; Junyusen, T.; Sutapun, W. Biogenic Vaterite Calcium Carbonate-Silver/Poly(Vinyl Alcohol) Film for Wound Dressing. *ACS Omega* **2024**, *9* (1), 955–969.

34.   Murphy, J. N.; Schneider, C. M.; Hawboldt, K.; Kerton, F. M. Hard to Soft: Biogenic Absorbent Sponge-like Material from Waste Mussel Shells. *Matter* **2020**, *3* (6), 2029–2041.

35.   Gallardi, D. Effect of the Environment on Condition and Quality of Cultured Blue Mussels (*Mytilus Edulis*) with Reference to Culture Depth and Post-Harvest Practices. doctoral, Memorial University of Newfoundland, 2016. https://research.library.mun.ca/11938/.

36.   Gullo, M.; Verzelloni, E.; Canonico, M. Aerobic Submerged Fermentation by Acetic Acid Bacteria for Vinegar Production: Process and Biotechnological Aspects. *Process Biochem.* 2014, *49* (10), 1571–1579.

37.   Ewing, T. A.; Nouse, N.; Lint, M. van; Haveren, J. van; Hugenholtz, J.; Es, D. S. van. Fermentation for the Production of Biobased Chemicals in a Circular Economy: A Perspective for the Period 2022–2050. *Green Chem.* **2022**, 24 (17), 6373–6405.

38.   Merli, G.; Becci, A.; Amato, A.; Beolchini, F. Acetic Acid Bioproduction: The Technological Innovation Change. *Sci. Total Environ.* **2021**, 798, 149292.

39.   Segale, L.; Giovannelli, L.; Mannina, P.; Pattarino, F. Calcium Alginate and Calcium Alginate-Chitosan Beads Containing Celecoxib Solubilized in a Self-Emulsifying Phase. *Scientifica (Cairo)* **2016**, *2016*, 5062706.

40.   Hecht, H.; Srebnik, S. Structural Characterization of Sodium Alginate and Calcium Alginate. *Biomacromolecules* **2016**, *17* (6), 2160–2167.

41.   Kikuchi, A.; Kawabuchi, M.; Sugihara, M.; Sakurai, Y.; Okano, T. Pulsed Dextran Release from Calcium-Alginate Gel Beads. *JCR* **1997**, *47* (1), 21–29.

42.   Leal, D.; Matsuhiro, B.; Rossi, M.; Caruso, F. FT-IR Spectra of Alginic Acid Block Fractions in Three Species of Brown Seaweeds. *Carbohydr. Res.* **2008**, 343 (2), 308–316.

43.   Sánchez-Machado, D. I.; López-Cervantes, J.; Escárcega-Galaz, A. A.; Campas-Baypoli, O. N.; Martínez-Ibarra, D. M.; Rascón-León, S. Measurement of the Degree of

Deacetylation in Chitosan Films by FTIR, ^{1}H NMR and UV Spectrophotometry. *MethodsX* **2024**, 12, 102583.

44.   Van de Velde, K.; Kiekens, P. Structure Analysis and Degree of Substitution of Chitin, Chitosan and Dibutyrylchitin by FT-IR Spectroscopy and Solid State ^{13}C NMR. *Carbohydr. Polym.* **2004**, 58 (4), 409–416.

45.   Christian-Robinson, S.; Kerton, F. M. One Story as Part of the Global Conversation on Sustainability: Dye Adsorption Studies Using a Novel Bio-Derived Calcite Material. *Pure Appl. Chem.* **2024**, 96, 1247-1255.